HHS Public Access

Author manuscript

Dig Dis Sci. Author manuscript; available in PMC 2015 July 23.

Published in final edited form as:

Dig Dis Sci. 2014 June ; 59(6): 1197–1206. doi:10.1007/s10620-014-3167-6.

Caspase 3 inactivation protects against hepatic cell death and ameliorates fibrogenesis in a diet induced NASH model

Samjhana Thapaliya[1,*], **Alexander Wree**[2,*], **Davide Povero**[2], **Maria Eugenia Inzaugarat**[2], **Michael Berk**[1], **Laura Dixon**[1], **Bettina G. Papouchado**[3], and **Ariel E Feldstein**[2]

[1]Department of Cellular and Molecular Medicine Lerner Research Institute Cleveland Clinic, Cleveland, Ohio, USA

[2]Department of Pediatrics, University of California – San Diego, 9500 Gilman Drive, La Jolla, CA, USA

[3]Department of Pathology, University of California San Diego, La Jolla, CA, USA

Abstract

Background/Aims—Hepatocyte cell death is a key feature of nonalcoholic steohepatitis (NASH). As the contribution of specific caspases remains unclear, our aim was to ascertain the effect of caspase 3 suppression on liver injury and fibrogenesis.

Methods—C57BL/6 wild-type (WT), and caspase 3 knock out (*Casp3*$^{-/-}$) mice were placed on a methionine- and choline-deficient (MCD) diet for 6 weeks to induce steatohepatitis and liver fibrosis. Thereafter, liver injury, liver fibrosis and hepatocellular apoptosis were quantified in liver sections. Additionally, expression of proteins associated with liver inflammation and fibrogenesis were analyzed.

Results—WT mice fed MCD diet showed marked activation of caspase 3 in hepatocytes, in conjunction with steatohepatitis and increased hepatic triglyceride levels, hepatocyte ballooning, inflammation and fibrosis. *Casp3*$^{-/-}$ fed the MCD diet showed similar serum ALT levels and NAFLD activity scores (NAS) compared to WT MCD-fed mice. However *Casp3*$^{-/-}$ mice on the MCD diet showed a marked reduction in expression of transcripts for pro-fibrogenic genes i which translated into reduced hepatic collagen deposition. These changes were associated with decreased levels of apoptosis, and a significant reduction in the expression of cytokines involved in inflammatory signaling. *Casp3*$^{-/-}$ mice on the MCD showed a reduction in expression of chemokine receptor 2 (CCR2) leading to ameliorated infiltration of inflammatory lymphocyte antigen 6 complex, locus C1 (Ly6c) positive monocytes.

Conclusion—These findings support a prominent role for hepatocyte caspase 3 activation in NASH related apoptosis, fibrogenesis and fibrosis which in part is mediated via CCR2 dependent infiltration of Ly6c positive monocytes.

Corresponding author: Ariel E. Feldstein, M. D., Professor of Pediatrics, Department of Pediatrics, University of California San Diego, 9500 Gilman Drive, MC 0715, La Jolla, CA. 92037-0715, USA, Tel: + 1 858 966 8907, Fax: + 1 858 966 8917, afeldstein@ucsd.edu.

*These authors contributed equally to this work

Financial Disclosures: None

Keywords

nonalcoholic fatty liver disease; caspases; apoptosis; liver injury; liver fibrosis

Introduction

Nonalcoholic Fatty Liver Disease (NAFLD) is currently the most common form of chronic liver disease in the Western World affecting both adults and children, and is strongly associated with obesity and insulin resistance [1, 2]. Hepatic steatosis, a stage within the spectrum of NAFLD that is characterized by triglyceride accumulation in liver cells and follows a benign non-progressive clinical course, is present in one out of three adults and one in ten children or adolescents in the United States [3, 4]. Some patients exhibit lipid accumulation with evidence of cellular damage, inflammation and different degrees of scarring or fibrosis which is commonly referred as Nonalcoholic steatohepatitis (NASH) [5]. Several studies have shown that NASH is a serious condition with approximately 25% of affected patients progressing to cirrhosis and being in danger of its associated complications: portal hypertension, liver failure and hepatocellular carcinoma [6–8].

Since the original description that caspase activation, and apoptotic cell death are characteristic pathologic features in the liver of NASH patients [9], increasing amount of data have demonstrated that hepatocyte cell death is a key process involved in NASH pathogenesis [10]. Caspases belong to a family of highly conserved cysteine-dependent aspartate-specific acid proteases that use a cysteine residue as catalytic nucleophile and share a stringent specificity for cleaving their substrates after aspartic acid residues in target proteins [11]. They are synthesized as inert zymogens and upon receipt of apoptotic stimuli, cells activate initiator caspases such as, caspase-1, -2, -8, -9, and -10 that, in turn, proteolytically cleave and activate effector caspases including caspase-3, -6, and -7 [12]. Caspases have been further categorized as either proinflammatory or proapoptotic, depending upon their participation in these cellular responses. Caspase 3, the prototype of a prodeath caspase, plays a central role in the apoptotic machinery [13]. In this process caspase 3 recognizes four contiguous amino acids (designated P4-P3-P2-P1-P1’) and cleaves the peptide bond between the P1-P1’ residues [14, 15].

The relative contribution of pro-apoptotic versus pro-inflammatory caspases to liver pathology during NASH development, as well as in the protective effects of pan-caspase inhibitors, remain incompletely understood. Given its central role in apoptosis, blocking caspase activity is now widely used as a therapeutic and diagnostic approach for several diseases, including NASH [16–19]. Recent studies have demonstrated that pan-caspase inhibition prevents the development of steatohepatitis [20–22]. Taking into account that caspase 3 has been identified to be the main player of apoptotic cell death we examined the effects of selective inactivation of caspase 3 during progression of steatohepatitis and fibrosis in vivo, and the cross-talk between hepatocytes and hepatic stellate cells (HSC) in vitro during lipotoxicity.

Methods

Animal Studies

The experimental protocols were approved by the Institutional Animal Care and Use Committee at the Cleveland Clinic. Caspase 3 knockout mice (*Casp3*$^{-/-}$) were generously provided by Dr. Mina Woo (University of Toronto). These mice were generated by deleting exon 3 of the CPP32/caspase 3 gene as previously described in detail [20]. They appear healthy and do not have a particular phenotype, but they do have a slightly decrease in life span. Casp3$^{-/-}$ and their wild-type controls, 20 to 25 gm of body weight, 7 weeks old, were placed on a methionine and choline-deficient (MCD) diet (TD 90262, Teklad Mills, Madison, WI), which has been extensively shown to result in steatosis associated with significant inflammation and progressive fibrosis pathologically similar to human severe steatohepatitis [21, 22] or a control diet (CTL) consisting of 5% fat (TD 2918, Teklad Mills, Madison, WI) to act as controls (n = 4–6 in each group). Animals in each group were sacrificed after 6 weeks on the respective diets and their liver tissue and plasma were collected under deep anesthesia as previously described in detail [16].

Histopathology, immunohistochemistry and serum assays

Liver tissue was fixed in 4% paraformaldehyde and embedded in Tissue Path (Fisher Scientific, Pittsburgh, PA, USA). Tissue sections (4 μm) were prepared, and hematoxylin and eosin, as well as Oil Red O stained liver specimens were evaluated by light microscopy. Individual features including degree of steatosis, inflammation, and ballooning were assessed in MCD and CTL-fed animals by an experienced pathologist (BGP) in a blinded fashion. Steatosis, inflammation, and ballooning were scored based on NAFLD activity score [23]. Serum alanine aminotransferase (ALT) determinations were performed using a commercial kit (Sigma Diagnostics, St. Louis, MO, USA). Liver triglycerides were quantified using a specific kit following manufacturer's instructions (Pointe Scientific, Canton, MI, USA). Immunohistochemistry for hepatic macrophages (F4/80, AbD Serotec, Raleigh, NC, USA) was performed in formalin-fixed, paraffin-embedded livers according to manufacturer’s instructions. Immunohistochemistry for lymphocyte antigen 6 complex, locus C1 (Ly6c) (Abcam, Cambrigde, MA, USA) was performed on frozen liver sections.

Apoptosis and Caspase-3 assessment

Terminal deoxynucleotidyl transferase dUTP nick-end labeling (TUNEL) assay was performed following manufacturer’s instructions (in-situ cell death detection kit; Roche Molecular Biochemicals, Mannheim, Germany). Hepatocyte apoptosis in liver sections was quantified by counting the number of TUNEL-positive cells in five random microscopic fields (40X), as previously described (28). Caspase activation was quantified using biochemical and immunohistochemical techniques: Caspase-Glo 3/7 Assay (Promega, Madison, WI, USA); immunostaining for active caspase 3 was performed using an antibody specific for the detection of cleaved caspase 3 (Cell Signaling, Boston, MA, USA).

Determination of liver fibrosis

Liver fibrosis was assessed using Sirius Red staining and α-smooth muscle actin (α-SMA) immunofluorescence. Direct Red 80 and Fast Green FCF (color index 42053) were provided by Sigma-Aldrich. Liver sections were incubated in the dark for 2 hours at room temperature with an aqueous solution of saturated picric acid containing 0.1% Direct Red. Stained slides were washed slowly under running distilled water for 6 minutes, dehydrated (3 minutes for each step), mounted, and examined by light microscopy. Red-stained collagen fibers were quantitated by digital image analysis. Immunofluorescence for α-SMA (Sigma) was performed on paraffin-embedded liver tissue using standard DAB technique (Vector, Burlingame, CA, USA) following manufacturer's instructions.

Real-Time PCR

Total RNA was isolated from liver tissue using RNeasy Lipid Tissue Mini kit (Qiagen, Valencia, CA). Reverse transcript (the cDNA) was synthesized from 1μg total RNA using iScript cDNA Synthesis Kit (Bio-Rad, Hercules, CA). Real-time PCR quantification was performed. Briefly, 25μl reaction mix contained: cDNA, SYBR Green buffer, Gold Taq polymerase, dNTPs and primers at final concentration of 200μM. Primers sequences used for quantitative PCR are given in supplementary table 1. RT-PCR was performed in the Mx3000P cycler (Stratagene): 95°C for 10 minutes, 40 cycles of 15 seconds at 95°C, 30 seconds at 60°C, 30 seconds at 72°C followed by a 1 minute at 95°C, 30 seconds at 55°C and 30 seconds at 95°C. The fold change over control samples was calculated using CT, ΔCT and ΔΔCT values using MxPro software (Stratagene). 18S ribosomal RNA (Ambion Inc, Austin, TX) was used as an endogenous control.

Western Blot

For immunoblot analysis 30mg whole liver lysate was resolved by a 4–20% gradient gel, transferred to nitrocellulose membrane, and blotted with an anti-α-SMA (GeneTex, Irvine, CA, USA) antibody. Membranes were incubated with peroxidase-conjugated secondary antibody (dilution 1:10,000) (GeneTex, Irvine, CA, USA), protein bands were visualized with the enhanced chemiluminescence reagent and digitized using a CCD camera (ChemiDoc®, Biorad, Hercules, CA, USA). Expression intensity was quantified by ImageLab (Biorad). Protein load was verified with an α-tubulin antibody (dilution 1:10,000) (Hybridomabank, University of Iowa).

Statistical analysis

Analyses were performed with Graph Pad (version 5.03; Graph Pad, Graph Pad Software Inc., CA, USA). Unless otherwise stated, data are expressed as mean +/− SEM or as absolute number or percentage for categorical variables. Differences between groups were compared by ANOVA followed by a post hoc Bonferroni test to correct for multiple comparisons. Differences were considered to be statistically significant at $p < 0.05$.

Results

Caspase 3 activation is a prominent pathological feature in experimental NASH

To investigate the role of caspase activation in the pathogenesis of NASH, we initially placed C57BL/6 mice on the methionine and choline deficient (MCD) diet which has been extensively shown to be associated with progressive fibrosing steatohepatitis pathologically similar to human severe steatohepatitis [21, 22]. After 6 weeks on the respective diets we observed significant hepatic fat accumulation induced by MCD feeding (Fig. 1A), in conjunction with an increase in histological parameters of liver injury including hepatic inflammation, and hepatocyte ballooning. These changes were associated with a marked increase in the expression of cleaved caspase 3 which was primarily localized to hepatocytes showing a predominantly cytoplasmic staining pattern (Fig. 1A, B). The changes observed in the level of cleaved caspase 3 were accompanied by a significant increase in hepatic caspase 3 activity (Fig. 1C).

Caspase 3 suppression is associated with decreased hepatocellular damage, cell death, and pro-inflammatory signaling

Having established the presence of increased caspase activity in the liver of MCD fed mice, we next sought to investigate the role of caspase 3 during NASH development by using caspase 3 knockout mice (*Casp3*$^{-/-}$). We first investigated whether *Casp3*$^{-/-}$ mice are resistant to liver injury and inflammation. C57BL/6 wild-type, and *Casp3*$^{-/-}$ mice were placed on either a MCD diet, or control (CTL) diet (n = 5 in each group) for 6 wks. Wild type mice on MCD diet developed the full spectrum of NASH with steatosis, inflammation, hepatocellular ballooning, resulting in an average NAFLD activity score (NAS) of 4 (Fig 2A, D). Serum ALT levels were about 4 fold higher in WT and *Casp3*$^{-/-}$ mice on the MCD diet compared to animals fed the control diet. (Fig. 2C). Microscopic examination showed that WT mice developed significant predominantly macro vesicular steatosis and no change in knockout mice compared to WT on MCD diet (Fig. 2B). Consistent with these result, hepatic triglyceride levels were similarly elevated in both knockout and WT mice on the MCD diet compared to the control diet (Fig. 2E). We next quantified the amount of hepatocellular cell death present in the various groups of mice. Consistent with the significant caspase 3 activation found in the WT animals on the MCD diet, we observed increased TUNEL positive cells in these mice, but not in the livers of Casp3$^{-/-}$ mice fed the same diet (Fig. 3 A–B).

Dietary induced Ly6c positive monocyte infiltration is ameliorated in *Casp3*$^{-/-}$ mice

When we examined the inflammatory state of the liver at the molecular and cellular level, we found that the total number of Kupffer cells / macrophages (F4/80) and mRNA expression levels were comparable in both groups of animals on the MCD diet (Fig 4A, B). However, only wild type mice on MCD diet, and not *Casp3*$^{-/-}$, showed a significant increase in number and mRNA expression level of inflammatory lymphocyte antigen 6 complex, locus C1 (Ly6c) positive monocytes (Fig. 4C, D). We also found that the major mediator of Ly6c infiltration - the chemokine receptor 2 (CCR2) - was significantly increased in WT mice on MCD diet when compared to WT mice on control diet and those levels were also significantly greater than those of *Casp3*$^{-/-}$ mice on MCD diet (Fig. 4E).

Analysis of marker for M1/M2 macrophage polarization (M1: TNF-α and IL-6; M2: Arg1 and IL-10) revealed a marked reduction in mRNA levels of TNF- and IL-6 in the MCD-fed *Casp3*$^{-/-}$ mice compared to the WT animals on the MCD diet (Fig. 4F). The same pattern was observed in the analysis of arginase 1 (Arg1), while mRNA levels of IL10 were increased in both groups fed with MCD diet without significant difference (Fig. 4G).

Hepatic stellate cell (HSC) activation and collagen deposition from MCD diet are prevented by caspase 3 suppression

The differential findings observed in the Casp3$^{-/-}$ mice in several aspects of hepatocyte viability and inflammatory signaling, two events that have been linked to HSC activation, led us to further examine the role of caspase 3 in fibrogenesis and fibrosis induced by the MCD diet. While after six weeks on the MCD diet wild type animals showed an almost four-fold increase in collagen deposition as demonstrated by Sirius red staining of liver tissue coupled to quantitation by digitized image analysis when compared to the wild type animals on the control diet (Fig. 5A-B), these changes were completely blunted in the Casp3$^{-/-}$ mice (Fig. 5A-B). Similarly an increase level of α-SMA protein expression was detected by both Western blot analysis and immunofluorescence in WT MCD-fed mice but not in Casp3$^{-/-}$ MCD- fed mice compared to the animals on the control diet (Fig. 5C-D). In line with this, we also found that after six weeks on the MCD diet wild type animals showed a marked increase in the mRNA expression of various genes involved in HSC activation and fibrogenesis (Fig. 5E). mRNA level of COL1A1, α-SMA and TGFβ all were increased in MCD fed WT mice but were completely blunted in Casp3$^{-/-}$ mice on same diet (Fig. 5E). Taken together, these observations suggest that during NASH development, caspase 3 activity plays a central role in liver injury, and hepatic fibrosis.

Discussion

The principal findings of this study relate to the effects of specific caspase 3 activation during NASH development. Active caspase 3 was found to be more abundant in livers of WT mice fed with a dietary NASH model (MCD). Suppression of caspase 3 resulted in protection of hepatocellular damage, cell death, and pro-inflammatory signaling. Notably the recruitment of profibrotic inflammatory monocytes was ameliorated in caspase 3 knockout mice. This translated to a marked reduction in collagen deposition and development of liver fibrosis. Effects were found to be independent of hepatic triglyceride accumulation. The results of the current study demonstrate that caspase 3 activation in hepatocytes plays a central role in steatohepatitis and fibrosis.

The importance of caspase activation and hepatocytes undergoing apoptosis in the liver of NASH patients has been described more than a decade ago [9], since then a growing number of studies have demonstrated that hepatocyte cell death is a key process involved in NASH pathogenesis [10]. Previous studies showed that both fundamental pathways of apoptosis, the so call extrinsic (death receptor mediated) pathway and the intrinsic (organelle-initiated) pathway contribute to the development of NASH in mice [24, 25]. Although the relative importance or predominance of these two pathways in human NASH remains to be elucidated, in hepatocytes, both tend to converge at the level of the mitochondria resulting in

permeabilization of the mitochondrial outer membrane and release of multiple proteins from the mitochondrial intermembrane space into the cytosol [26–28].

A central consequence of this process is the activation of the effector caspases (mainly caspase 3) which will then cleaved a number of different substrates inside the cell resulting in the characteristic morphologic changes of apoptosis [29, 30]. Targeting caspase activity has gained significant attention for developing of both novel therapeutic and diagnostic strategies for NASH patients. Three independent pre-clinical studies using different models of dietary induced NASH in mice showed significant protective effects of pan-caspase inhibitors in both parameters of inflammation as well as fibrosis [31–33].

A key question extant is whether suppression of the effector caspase 3 in NASH would result in a switch to caspase 3-independent cell death and thus no protection or even worsening of the liver disease by inducing a compensatory increased in necrotic cell death may occur. Our study demonstrates that caspase 3 suppression does not improve steatosis, histological inflammatory scores parameters or decrease serum ALT levels in this mouse model of NASH. However, MCD-fed Casp3$^{-/-}$ mice showed a reduction in indices of hepatocellular damage such as ballooning of hepatocytes, decrease level of apoptosis, marked decrease in pro-inflammatory signaling, and reduced infiltration of inflammatory macrophages. Although based on observations on developing animals, and in vitro studies in immortalized cell lines, apoptosis has been perceived to be non-inflammatory, it has become apparent that pathological increase in apoptosis in the context of chronic diseases may directly or indirectly promote inflammation [34, 35]. The current data extends these observations and demonstrate that the protection from hepatocyte apoptosis seen on the caspase 3 knockout mice was associated with a marked decrease in pro-inflammatory cytokines levels in liver tissue and infiltration of Ly6c inflammatory monocytes. It is known that sustained inflammation upon chronic liver injury mainly induces the development of liver fibrosis with recent studies showing that liver-resident macrophages only partially conducted these actions but largely depends on recruitment of monocytes into the liver [36–38]. Upon organ injury, chemokine receptor CCR2 promote monocyte subset accumulation in the liver, namely of the inflammatory Ly6C+ (Gr1+) monocyte subset as precursors of tissue macrophages [39, 40]. In the present study we are able to show that MCD induced increase in CCR2 expression and recruitment of Ly6c positive macrophages is ameliorated in Casp3$^{-/-}$ mice.

Another important aspect of blocking caspase 3 activation is the fact that this protease might be required for apoptosis of activated HSC which has been proposed as a potential mechanism to limit fibrogenesis and thus inhibition of such a process could hypothetically result in fibrosis progression. While, as expected after six weeks on the MCD diet wild type animals showed a marked increase in the expression of various genes involved in HSC activation and fibrogenesis, these changes were significantly reduced in the Casp3$^{-/-}$ mice. More importantly, an almost four-fold increase in collagen deposition was present in wild-type animals on the MCD diet, and these changes were completely blunted in the Casp3$^{-/-}$ mice. Thus, the results of the current study suggest that inhibiting caspase 3 activation in hepatocytes significantly impact the production of pro-inflammatory cytokines such as TNF- and IL-6 and prevents HSC activation and fibrosis development. Moreover, these results

supports the concept that caspase 3 activation in parenchymal cells is a key stimulus for HSC activation and fibrosis and overpowers the potential fibrotic effects of caspase 3-independent cell death as well as the putative antifibrotic effect of HSC apoptosis induction. Future studies such as those using cell-type specific caspase-3 knockout mice will be required to further dissect the role of caspase-3 activation in hepatocyte versus non-parenchymal cells of the liver in vivo and their potential distinct role in the pathophysiologic changes observed during NASH development. In summary, the current studies uncover the role of hepatic caspase 3 activation in experimental NASH. The results support a model in which during the development of NASH, lipotoxicity triggers caspase 3 activation in hepatocytes, resulting in hepatocellular damage and steatohepatitis development. Caspase 3 activation further induces the release of signals that activates HSC resulting in fibrogenesis and eventually fibrosis. These data have significant implications for development of potential targets for therapeutic intervention.

Supplementary Material

Refer to Web version on PubMed Central for supplementary material.

Acknowledgments

This work was supported by NIH grants (DK076852) and (DK082451) to AEF.

References

1. Wieckowska A, Feldstein AE. Nonalcoholic fatty liver disease in the pediatric population: a review. Current opinion in pediatrics. 2005; 17:636–641. [PubMed: 16160540]
2. Angulo P. Nonalcoholic fatty liver disease. The New England journal of medicine. 2002; 346:1221–1231. [PubMed: 11961152]
3. Browning JD, Szczepaniak LS, Dobbins R, et al. Prevalence of hepatic steatosis in an urban population in the United States: impact of ethnicity. Hepatology. 2004; 40:1387–1395. [PubMed: 15565570]
4. Schwimmer JB, Deutsch R, Kahen T, Lavine JE, Stanley C, Behling C. Prevalence of fatty liver in children and adolescents. Pediatrics. 2006; 118:1388–1393. [PubMed: 17015527]
5. Wieckowska A, Feldstein AE. Diagnosis of nonalcoholic fatty liver disease: invasive versus noninvasive. Seminars in liver disease. 2008; 28:386–395. [PubMed: 18956295]
6. Adams LA, Lymp JF, St Sauver J, et al. The natural history of nonalcoholic fatty liver disease: a population-based cohort study. Gastroenterology. 2005; 129:113–121. [PubMed: 16012941]
7. Matteoni CA, Younossi ZM, Gramlich T, Boparai N, Liu YC, McCullough AJ. Nonalcoholic fatty liver disease: a spectrum of clinical and pathological severity. Gastroenterology. 1999; 116:1413–1419. [PubMed: 10348825]
8. Ekstedt M, Franzen LE, Mathiesen UL, et al. Long-term follow-up of patients with NAFLD and elevated liver enzymes. Hepatology. 2006; 44:865–873. [PubMed: 17006923]
9. Feldstein AE, Canbay A, Angulo P, et al. Hepatocyte apoptosis and fas expression are prominent features of human nonalcoholic steatohepatitis. Gastroenterology. 2003; 125:437–443. [PubMed: 12891546]
10. Cazanave SC, Gores GJ. Mechanisms and clinical implications of hepatocyte lipoapoptosis. Clinical lipidology. 2010; 5:71–85. [PubMed: 20368747]
11. Li J, Yuan J. Caspases in apoptosis and beyond. Oncogene. 2008; 27:6194–6206. [PubMed: 18931687]
12. Weber IT, Fang B, Agniswamy J. Caspases: structure-guided design of drugs to control cell death. Mini Rev Med Chem. 2008; 8:1154–1162. [PubMed: 18855730]

13. Pop C, Salvesen GS. Human caspases: activation, specificity, and regulation. J Biol Chem. 2009; 284:21777–21781. [PubMed: 19473994]
14. Earnshaw WC, Martins LM, Kaufmann SH. Mammalian caspases: structure, activation, substrates, and functions during apoptosis. Annual review of biochemistry. 1999; 68:383–424.
15. Fuentes-Prior P, Salvesen GS. The protein structures that shape caspase activity, specificity, activation and inhibition. The Biochemical journal. 2004; 384:201–232. [PubMed: 15450003]
16. Feldstein A, Gores GJ. Steatohepatitis and apoptosis: therapeutic implications. The American journal of gastroenterology. 2004; 99:1718–1719. [PubMed: 15330908]
17. Wieckowska A, Zein NN, Yerian LM, Lopez AR, McCullough AJ, Feldstein AE. In vivo assessment of liver cell apoptosis as a novel biomarker of disease severity in nonalcoholic fatty liver disease. Hepatology. 2006; 44:27–33. [PubMed: 16799979]
18. Hatting M, Zhao G, Schumacher F, et al. Hepatocyte caspase-8 is an essential modulator of steatohepatitis in rodents. Hepatology. 2013; 57:2189–2201. [PubMed: 23339067]
19. Dixon LJ, Flask CA, Papouchado BG, Feldstein AE, Nagy LE. Caspase-1 as a central regulator of high fat diet-induced non-alcoholic steatohepatitis. PloS one. 2013; 8:e56100. [PubMed: 23409132]
20. Woo M, Hakem R, Soengas MS, et al. Essential contribution of caspase 3/CPP32 to apoptosis and its associated nuclear changes. Genes & development. 1998; 12:806–819. [PubMed: 9512515]
21. Nanji AA. Animal models of nonalcoholic fatty liver disease and steatohepatitis. Clinics in liver disease. 2004; 8:559–574. ix. [PubMed: 15331064]
22. Koteish A, Diehl AM. Animal models of steatosis. Seminars in liver disease. 2001; 21:89–104. [PubMed: 11296700]
23. Kleiner DE, Brunt EM, Van Natta M, et al. Design and validation of a histological scoring system for nonalcoholic fatty liver disease. Hepatology. 2005; 41:1313–1321. [PubMed: 15915461]
24. Alkhouri N, Dixon LJ, Feldstein AE. Lipotoxicity in nonalcoholic fatty liver disease: not all lipids are created equal. Expert Rev Gastroenterol Hepatol. 2009; 3:445–451. [PubMed: 19673631]
25. Feldstein AE, Gores GJ. Apoptosis in alcoholic and nonalcoholic steatohepatitis. Front Biosci. 2005; 10:3093–3099. [PubMed: 15970563]
26. Li Z, Berk M, McIntyre TM, Gores GJ, Feldstein AE. The lysosomal-mitochondrial axis in free fatty acid-induced hepatic lipotoxicity. Hepatology. 2008; 47:1495–1503. [PubMed: 18220271]
27. Feldstein AE, Canbay A, Guicciardi ME, Higuchi H, Bronk SF, Gores GJ. Diet associated hepatic steatosis sensitizes to Fas mediated liver injury in mice. J Hepatol. 2003; 39:978–983. [PubMed: 14642615]
28. Feldstein AE, Werneburg NW, Canbay A, et al. Free fatty acids promote hepatic lipotoxicity by stimulating TNF-alpha expression via a lysosomal pathway. Hepatology. 2004; 40:185–194. [PubMed: 15239102]
29. Green DR. Apoptotic pathways: ten minutes to dead. Cell. 2005; 121:671–674. [PubMed: 15935754]
30. Chowdhury I, Tharakan B, Bhat GK. Caspases - an update. Comp Biochem Physiol B Biochem Mol Biol. 2008; 151:10–27. [PubMed: 18602321]
31. Barreyro F, Holod S, Finocchietto P. PF-03491390 Pan-caspase inhibitor decreases liver injury and fibrosis in a murine model of non-alcoholic steatohepatitis (NASH). Journal of hepatology. 2010; 52:S303.
32. Witek RP, Stone WC, Karaca FG, et al. Pan-caspase inhibitor VX-166 reduces fibrosis in an animal model of nonalcoholic steatohepatitis. Hepatology. 2009; 50:1421–1430. [PubMed: 19676126]
33. Anstee QM, Concas D, Kudo H, et al. Impact of pan-caspase inhibition in animal models of established steatosis and non-alcoholic steatohepatitis. Journal of hepatology. 2010; 53:542–550. [PubMed: 20557969]
34. Alkhouri N, Gornicka A, Berk MP, et al. Adipocyte apoptosis, a link between obesity, insulin resistance, and hepatic steatosis. The Journal of biological chemistry. 2010; 285:3428–3438. [PubMed: 19940134]

35. Syn WK, Choi SS, Diehl AM. Apoptosis and cytokines in non-alcoholic steatohepatitis. Clin Liver Dis. 2009; 13:565–580. [PubMed: 19818305]

36. Imamura M, Ogawa T, Sasaguri Y, Chayama K, Ueno H. Suppression of macrophage infiltration inhibits activation of hepatic stellate cells and liver fibrogenesis in rats. Gastroenterology. 2005; 128:138–146. [PubMed: 15633130]

37. Seki E, De Minicis S, Gwak GY, et al. CCR1 and CCR5 promote hepatic fibrosis in mice. The Journal of clinical investigation. 2009; 119:1858–1870. [PubMed: 19603542]

38. Tacke F. Functional role of intrahepatic monocyte subsets for the progression of liver inflammation and liver fibrosis in vivo. Fibrogenesis & tissue repair. 2012; 5(Suppl 1):S27. [PubMed: 23259611]

39. Karlmark KR, Weiskirchen R, Zimmermann HW, et al. Hepatic recruitment of the inflammatory Gr1+ monocyte subset upon liver injury promotes hepatic fibrosis. Hepatology. 2009; 50:261–274. [PubMed: 19554540]

40. Seki E, de Minicis S, Inokuchi S, et al. CCR2 promotes hepatic fibrosis in mice. Hepatology. 2009; 50:185–197. [PubMed: 19441102]

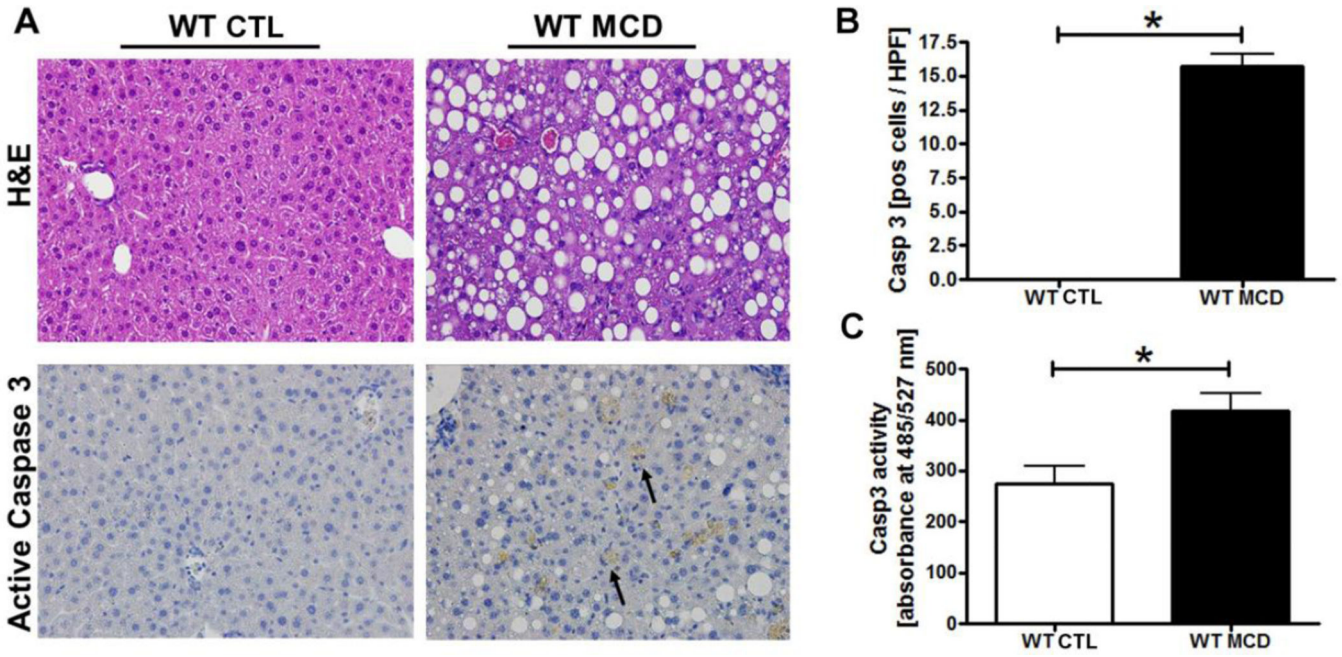

Fig. 1. MCD diet results in steatohepatitis development and marked hepatocyte caspase 3 activation

(A) Representative pictures of Hematoxylin & Eosin (H&E) staining and active caspase 3 immunohistochemistry of liver from the wild-type animals on the MCD or control diets (magnification 40x) and corresponding quantification (B). (C) Caspase 3 activation in the different groups of mice was assessed by Apo-ONE Homogeneous Caspase 3 fluorometric assays. Results are represented as mean ± SEM. * $P < 0.05$.

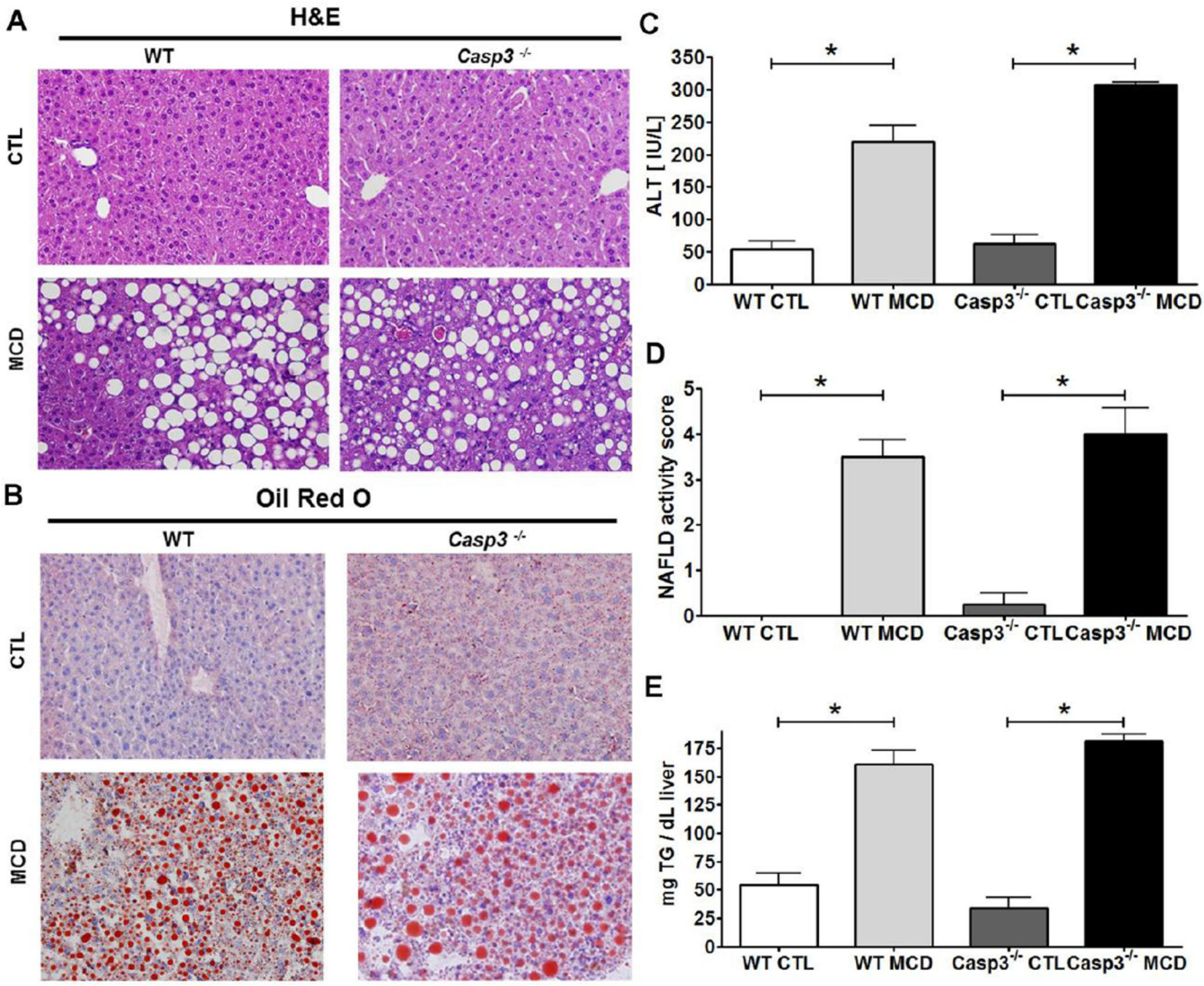

Fig. 2. Metabolic changes, histological features, hepatic triglyceride levels, and serum ALT levels in *Casp3*$^{-/-}$ and WT mice on the MCD and CTL diets

Male C57BL/6 mice (wild type), 20–25 g of body weight and C57BL/6 caspase 3 knockout (*Casp3*$^{-/-}$) were placed on either a control diet or methionine choline deficient (MCD) diet for 6 weeks. Histological microphotographs of Hematoxylin & Eosin (H&E), and (A) Oil red O stained liver sections of animals from the four different groups of mice (B) (magnification 40x). Serum ALT levels assessed at the time of sacrifice showed significantly increased level in mice fed with MCD regardless of the genetic background (C). NAFLD activity score also showed significantly increased level in mice fed with the methionine deficient diet (D) Hepatic triglyceride levels was assessed in all mice at the time of sacrifice and the mean ± SEM are graphed (E). Results are represented as mean ± SEM. * $P < 0.05$.

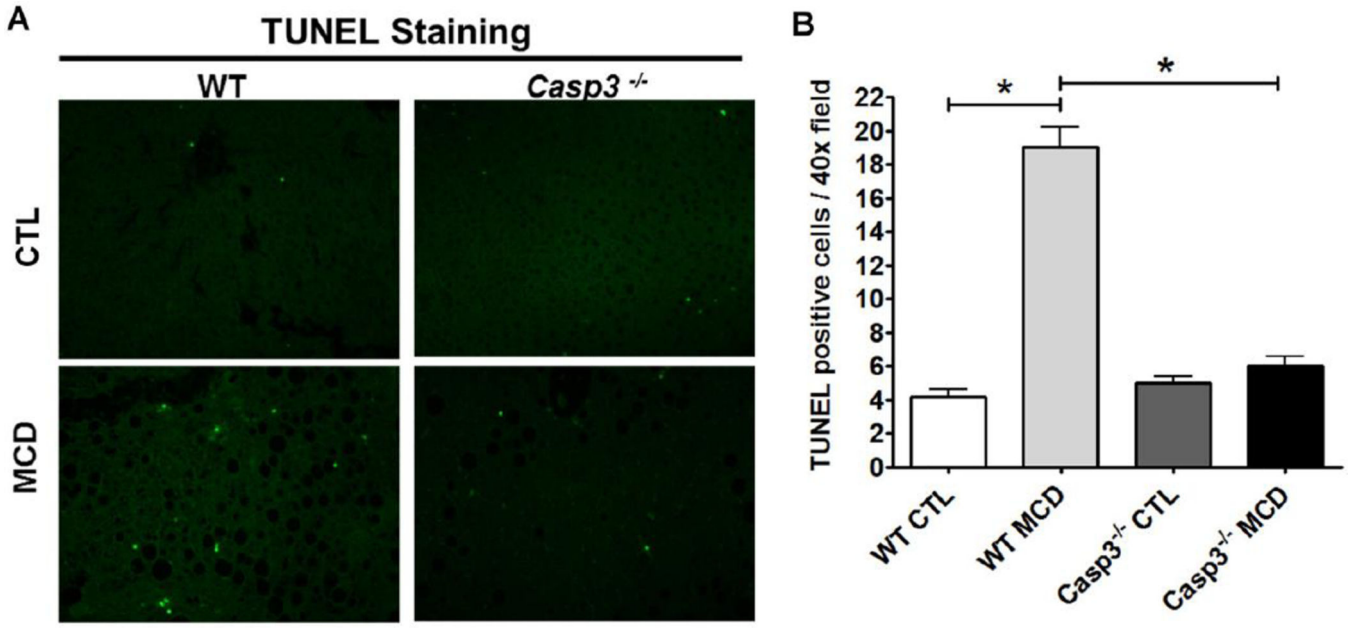

Fig. 3. Hepatocyte cell death is decrease in *Casp3*$^{-/-}$ mice compared to WT mice on MCD diet

Tissues were fixed in 4% paraformaldehyde and embedded in Tissue Path. Tissue sections (4 m) were prepared. (A) Representative images of Terminal deoxynucleotidyl transferase dUTP nick-end labeling (TUNEL) staining in the four groups of mice (magnification 40x). (B) Semi-quantification of TUNEL positive cells in *Casp3*$^{-/-}$ mice and WT mice on MCD diet normalized to CTL diet. Results are represented as mean ± SEM. * $P < 0.05$.

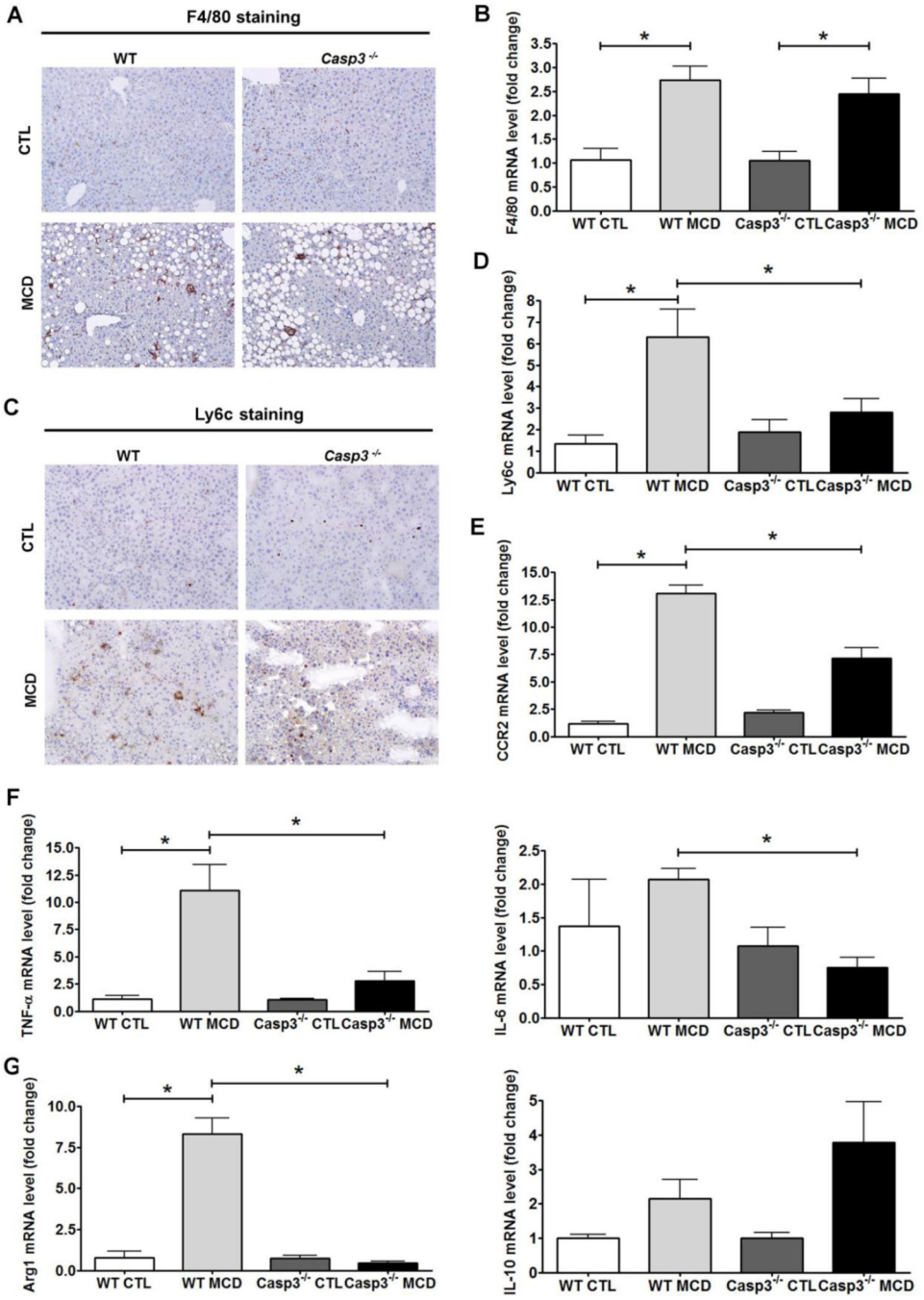

Fig. 4. *Casp3*$^{-/-}$ mice exhibit less Ly6c positive monocytes when compared to WT mice on MCD diet

The total number of Kupffer cells / macrophages (F4/80) (representative sections are shown in 20x magnification) and mRNA expression level were comparable in both groups of animals on the MCD diet (Fig 4A, B) and significantly greater when compared to mice on control diet. Expression levels and number of inflammatory lymphocyte antigen 6 complex, locus C1 (Ly6c) positive monocytes (representative sections are shown in 20x magnification)was only found to be increased in wild type mice on MCD diet and not

Casp3$^{-/}$ (Fig. 4C, D). Expression of chemokine receptor 2 (CCR2) was significantly increased in WT mice on MCD diet when compared to WT mice on control diet and those levels were also significantly greater than those of *Casp3*$^{-/-}$ mice on MCD diet (Fig. 4E). mRNA levels of TNF- and IL-6 were significantly reduced in MCD-fed *Casp3*$^{-/-}$ mice when compared to WT mice on the MCD diet (Fig. 4F). Expression levels of Arg1 followed the same pattern, whereas mRNA levels of IL10 were increased in both groups fed with MCD diet without significant difference (Fig. 4G).

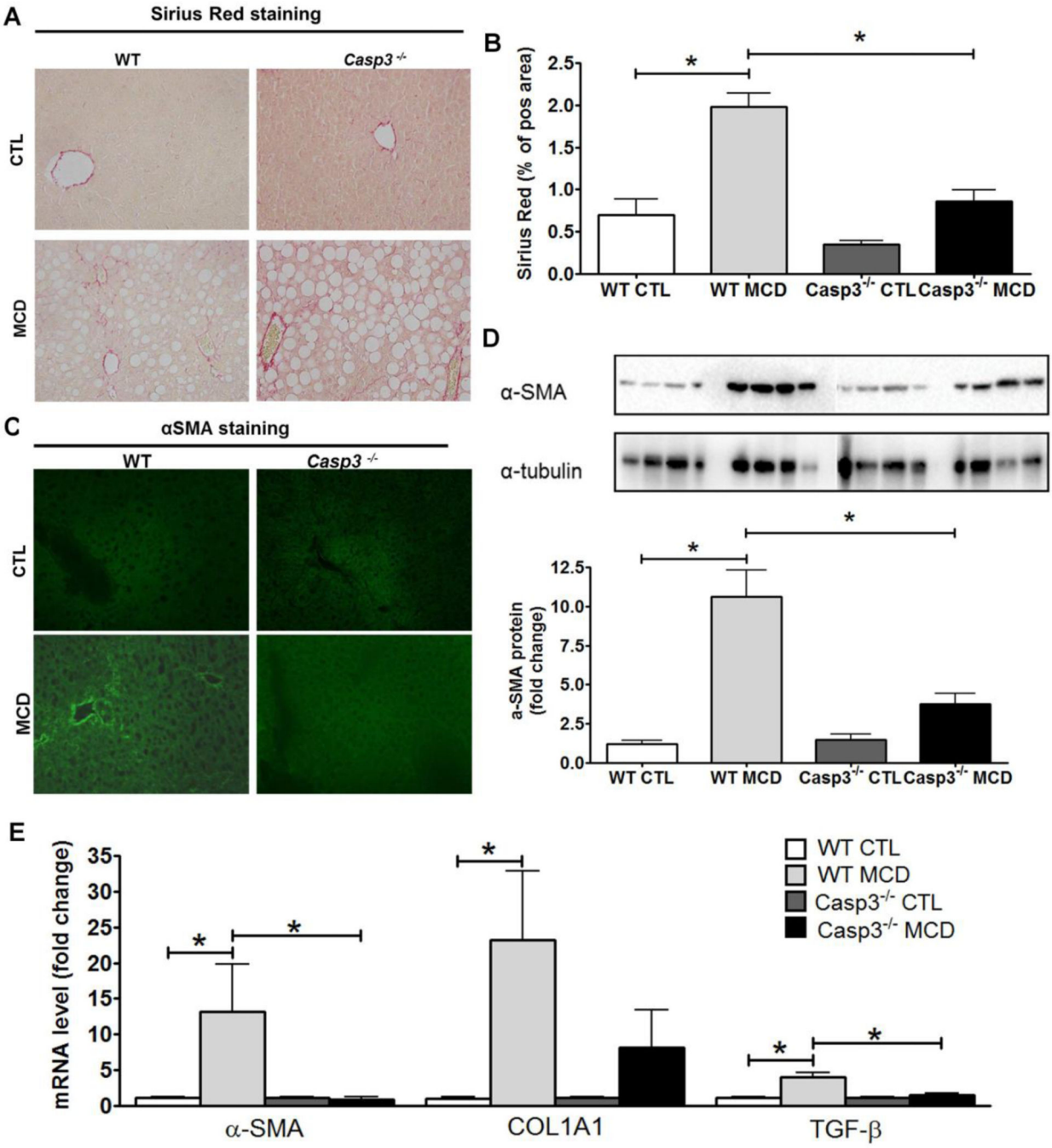

Fig. 5. Markers of HSC activation and collagen deposition are markedly decreased in Casp3$^{-/-}$ mice compared to WT mice on MCD diet

Quantification of collagen fibers was performed in liver section stained with Sirius red (A) (magnification 40x) and quantified using the surface area stained per field area ± S.D. (n = 4–6 in each group) excluding blood vessels (B). Immunofluorescence staining of α-SMA was also performed on frozen liver section (C). α-SMA was detected using western blot assay from liver homogenates and densitometry analysis of α-SMA over α-tubulin was analyzed (D). Quantitative RT PCR analysis of HSC activation markers alpha-smooth muscle actin (-SMA), collagen, type I-alpha (COL1A1), and transforming growth factor-

beta (TGF-) mRNA expression was assessed in WT and *Casp3*$^{-/-}$ mice on the CTL and MCD diet (n = 4–5 in each group). Results are expressed as mean ± SEM. *p-value < 0.05.